molecules

MDPI

Supplementary Material

In Silico Identification of Potential Sites for a Plastic-Degrading Enzyme by a Reverse Screening through the Protein Sequence Space and Molecular Dynamics Simulations

Krit Charupanit [1], Varomyalin Tipmanee [1], Thana Sutthibutpong [2,3] and Praopim Limsakul [4,5,*]

[1] Department of Biomedical Sciences and Biomedical Engineering, Faculty of Medicine, Prince of Songkla University, Songkhla 90110, Thailand; krit.ch@psu.ac.th (K.C.), tvaromya@medicine.psu.ac.th (V.T.)
[2] Theoretical and Computational Physics Group, Department of Physics, Faculty of Science, King Mongkut's University of Technology Thonburi (KMUTT), Bangkok 10140, Thailand; thana.sut@kmutt.ac.th
[3] Center of Excellence in Theoretical and Computational Science (TaCS-CoE), Faculty of Science, King Mongkut's University of Technology Thonburi (KMUTT), Bangkok 10140, Thailand
[4] Division of Physical Science, Faculty of Science, Prince of Songkla University, Songkhla 90110, Thailand
[5] Center of Excellence for Trace Analysis and Biosensor (TAB-CoE), Faculty of Science, Prince of Songkla University, Songkhla 90110, Thailand
* Correspondence: praopim.l@psu.ac.th

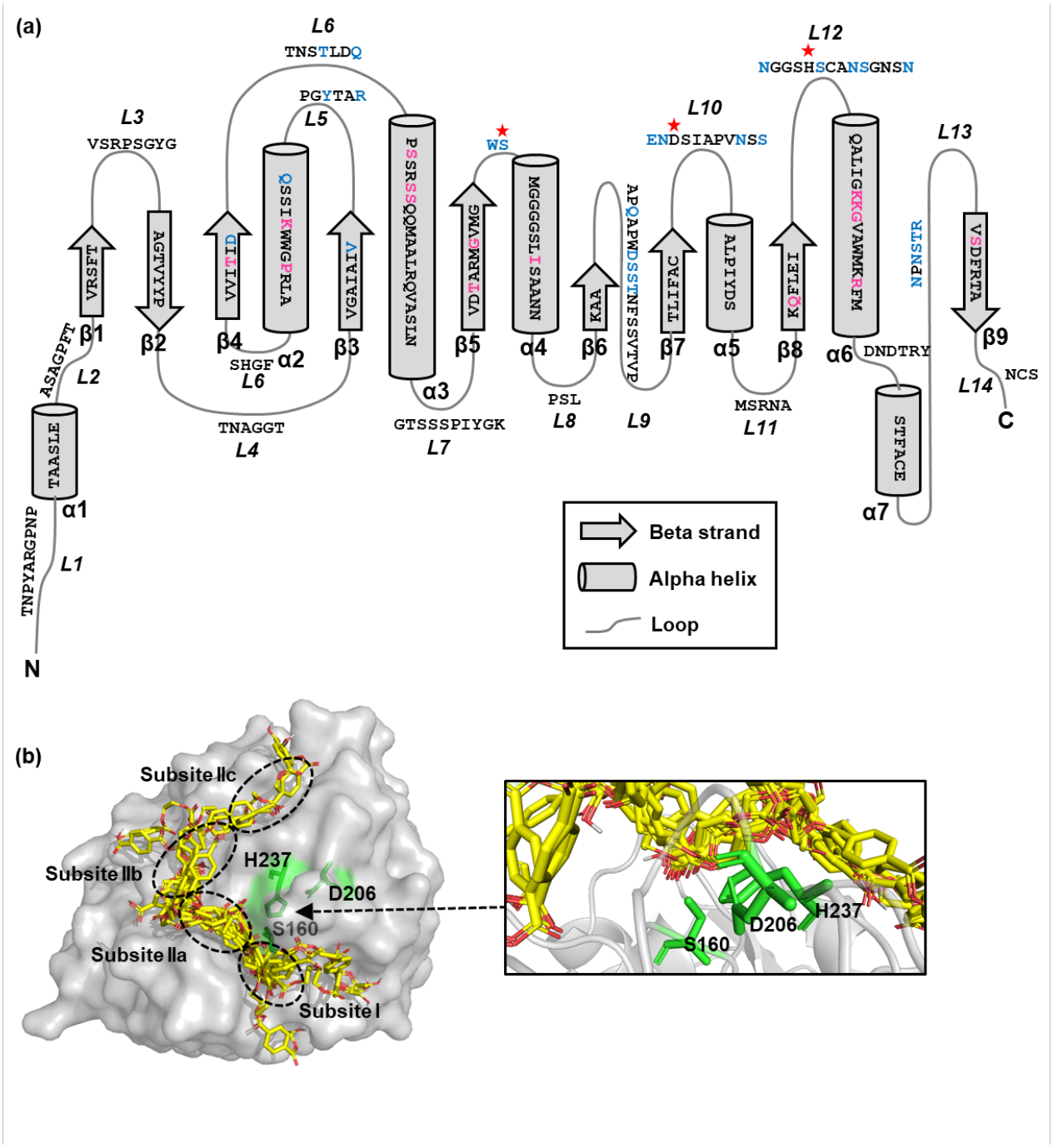

Figure S1. PETase structure and the active site of PETase. (**a**) Schematic representation of a PETase enzyme displaying the amino acid sequences on alpha helices, beta strands, and loops connecting pairs of secondary structures. Catalytic residues (S160, D206, and H237) are denoted by red stars. L represents a loop. (**b**) The docking poses of WT PETase and representative PETase variants, including Y87A, D112A, Q119A, N205A, S214A, S238A, R280A, and K253A. Left: The PETase structure is shown as a surface model with a gray color. The three residues forming a catalytic triad (S160, D206 and H237) are displayed as green-colored sticks. The PET substrate is shown as yellow-colored sticks. Right: Side view of the substrate binding mode of PETase at the active site. The L-shaped binding cleft, consisting of subsite I, IIa, IIb, and IIc, are indicated in the dash line.

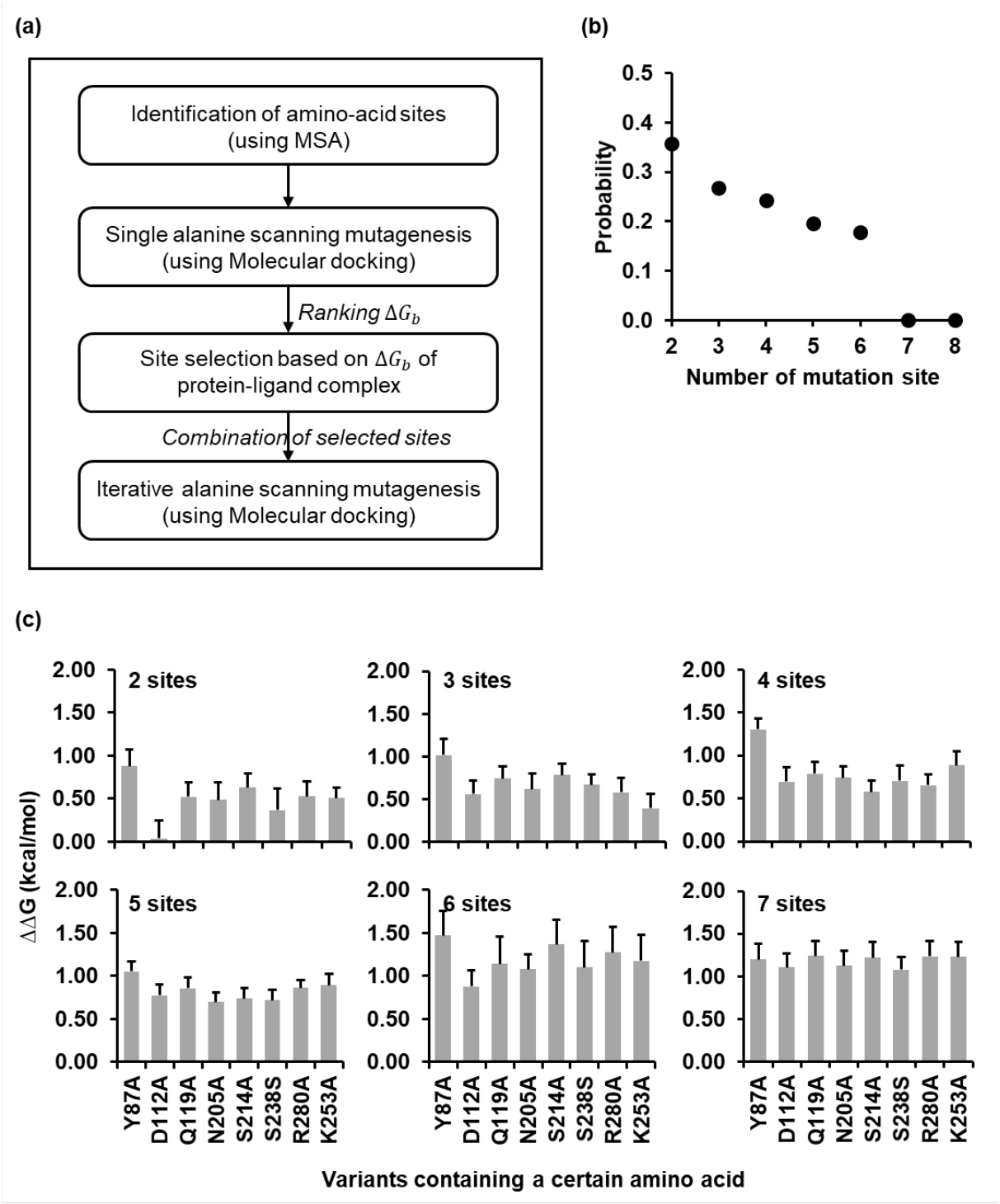

Figure S2. Results of iterative *in silico* alanine scanning mutagenesis. (**a**) Schematic diagram for iterative *in silico* ASM. Each step was performed in the sequencial format. (**b**) The probability of finding desired variants with different combination of mutaion sites. (**c**) The relation of selected amino acid sites and binding free energy with different numbers of mutation sites. The bar graphs show the average binding free energy difference (ΔΔG) of the PETase variant-PET complexes. Data are means ± S.D., where the mean is the average ΔΔG of all variants that contain the labeled amino acid.

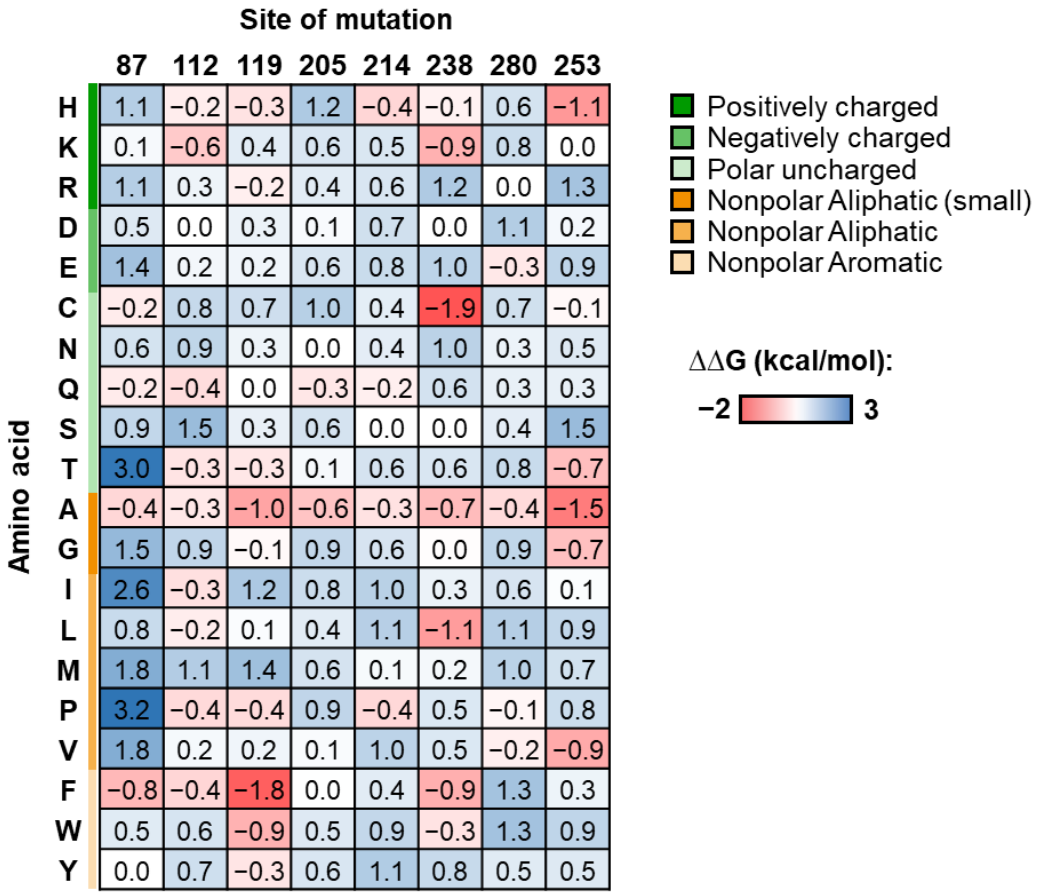

Figure S3. Effect of single site-saturation mutagenesis on the binding free energy. The one-dimension protein sequence space of PETase with different sites of mutation (positions 87, 112, 119, 205, 214, 238, 280, and 253). The color map displays the ΔΔG distribution where the blue color represents high ΔΔG (bad variant), and the red color represents low ΔΔG (good variant).

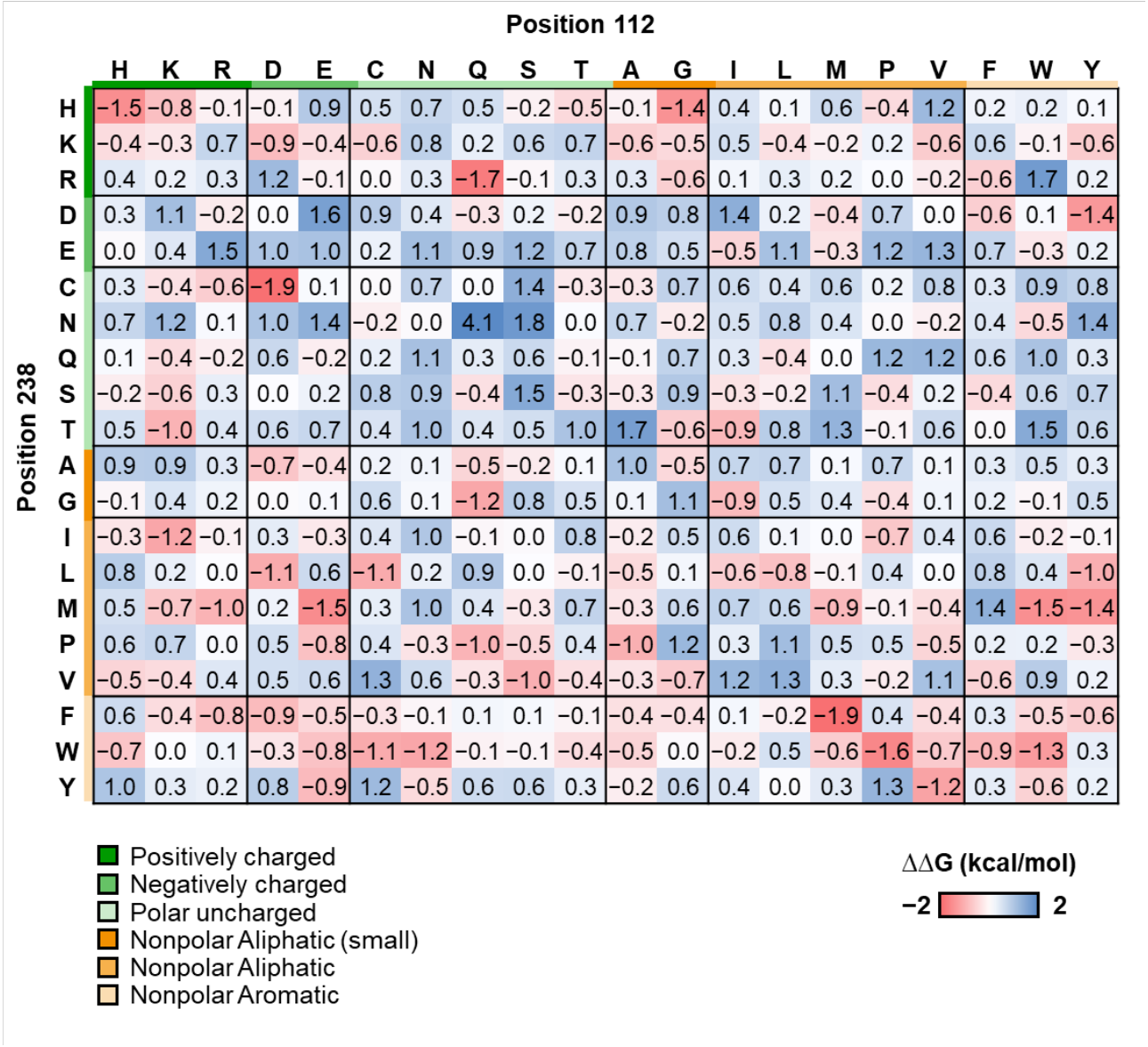

Figure S4. Effect of double site-saturation mutagenesis on the binding free energy. The two-dimension protein sequence space of PETase where the x- and y-axis represent amino acids at positions 112 and 238, respectively. Amino acids are categorized by their physicochemical properties, including positively charged, negatively charged, polar uncharged, non-polar small aliphatic, aliphatic, and aromatic. In the color bar, the blue color represents high ΔΔG (bad variant), and the red color represents low ΔΔG (good variant).

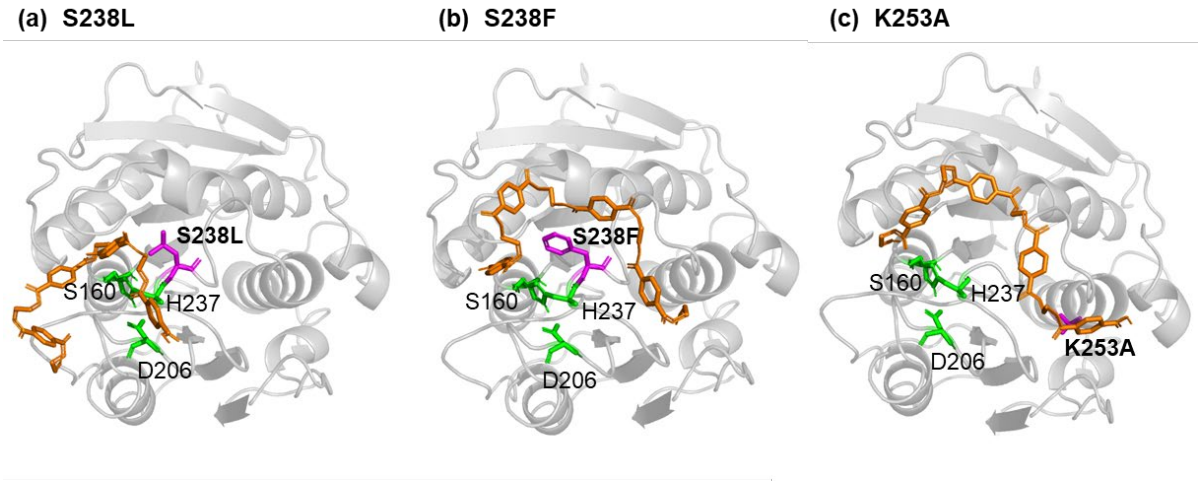

Figure S5. Docking poses of the PETase and PET complex. Three-dimensional ribbon representations of the PETase variants, including (**a**) S238L, (**b**) S238F, and (**c**) K253A, in the complex with the PET substrate were displayed. The catalytic triad, PET substrate docking model, and mutated residues were highlighted in green, orange, and magenta, respectively.

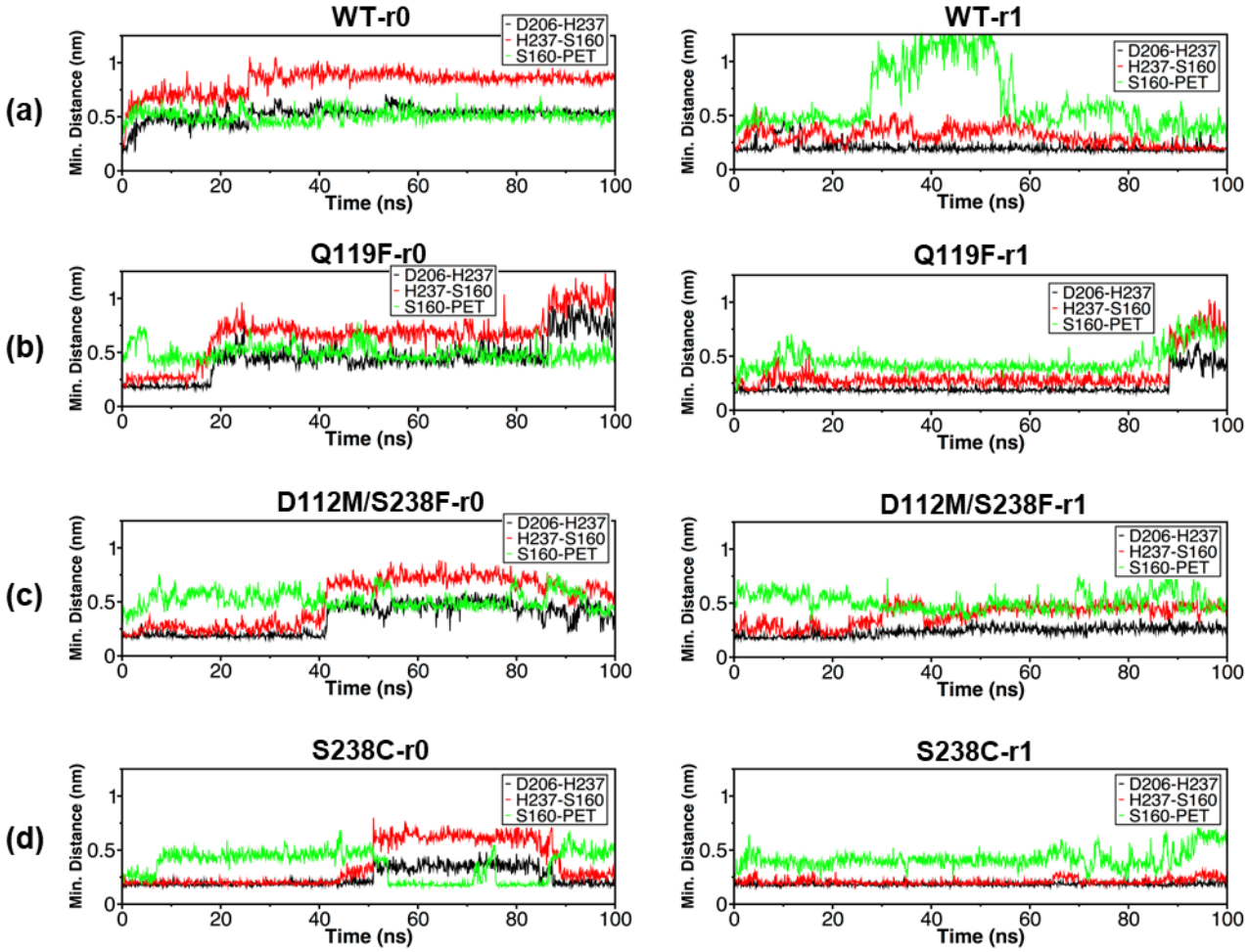

Figure S6. Minimum distances. Minimum distances calculated between the groups of atoms within D206 and H237 catalytic residues (black line), S160 and H237 catalytic residues (red line), and S160 and tetra-PET substrate (green line) are displayed in the following orders of (a) WT, (b) Q119F, (c) D112M/S238F, and (d) S238C with two replicas 'r0' (Left) and 'r1' (Right).

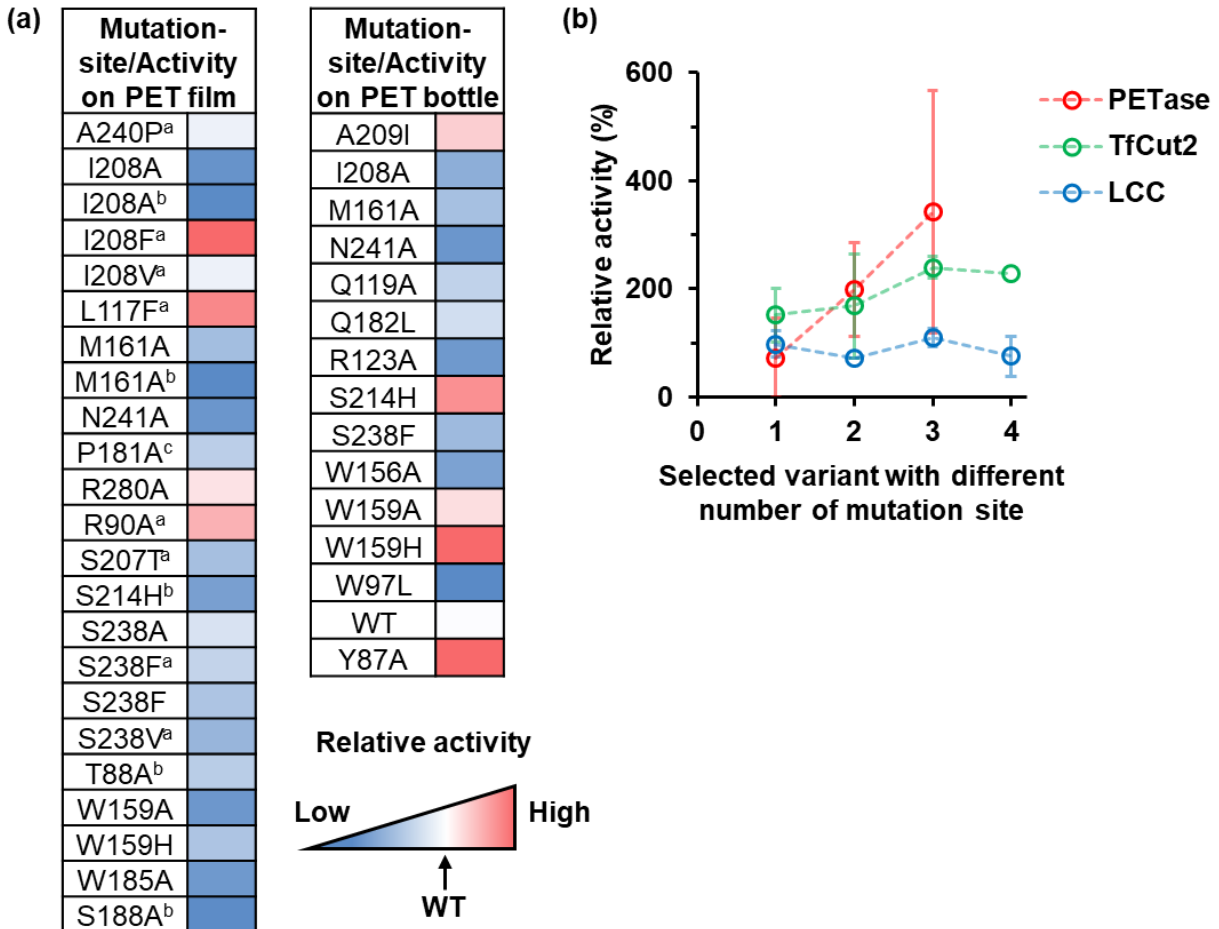

Figure S7. Experimental results of PET-degrading enzymes. (**a**) The PET-degrading activity of PETase variants with different mutation sites were tested either on PET film or in a PET bottle and compared with the wild-type PETase from the experiment. The color bar ranged from blue to red where the blue and red color represented lower and higher PET-degrading activity than the WT (white), respectively. (**b**) The graph shows the relation between the relative activity and the different number of mutation sites of PET-degrading enzymes such as PETase (red), TfCut2 (green), and LCC (blue). Data are mean ± S.D. All data in (A) for PET film (left table) were collected from [23], otherwise indicated, such as [a] [31], [b] [25], and [c] [32]. All data in (A) for PET bottle (right table) were collected from [24].

Table S1. All PETase variants and their mutation sites.

The table shows the alanine substituting combinations of each variant containing one to eight mutation sites (as indicated by the letters A to H) at positions 87, 112, 119, 205, 214, 238, 280, and 253 (as presented in each column). The gray color displays the combination of mutation sites of each variant. Variants that have the binding free energy lower than the WT (negative $\Delta\Delta G$) are highlighted in red rectangles.

Position	87	112	119	205	214	238	280	253	Position	87	112	119	205	214	238	280	253	Position	87	112	119	205	214	238	280	253	Position	87	112	119	205	214	238	280	253	Position	87	112	119	205	214	238	280	253
WT									C15									D10									D61									E42								
A1									C16									D11									D62									E43								
A2									C17									D12									D63									E44								
A3									C18									D13									D64									E45								
A4									C19									D14									D65									E46								
A5									C20									D15									D66									E47								
A6									C21									D16									D67									E48								
A7									C22									D17									D68									E49								
A8									C23									D18									D69									E50								
B1									C24									D19									D70									E51								
B2									C25									D20									E1									E52								
B3									C26									D21									E2									E53								
B4									C27									D22									E3									E54								
B5									C28									D23									E4									E55								
B6									C29									D24									E5									E56								
B7									C30									D25									E6									F1								
B8									C31									D26									E7									F2								
B9									C32									D27									E8									F3								
B10									C33									D28									E9									F4								
B11									C34									D29									E10									F5								
B12									C35									D30									E11									F6								
B13									C36									D31									E12									F7								
B14									C37									D32									E13									F8								
B15									C38									D33									E14									F9								
B16									C39									D34									E15									F10								
B17									C40									D35									E16									F11								
B18									C41									D36									E17									F12								
B19									C42									D37									E18									F13								
B20									C43									D38									E19									F14								
B21									C44									D39									E20									F15								
B22									C45									D40									E21									F16								
B23									C46									D41									E22									F17								
B24									C47									D42									E23									F18								
B25									C48									D43									E24									F19								
B26									C49									D44									E25									F20								
B27									C50									D45									E26									F21								
B28									C51									D46									E27									F22								
C1									C52									D47									E28									F23								
C2									C53									D48									E29									F24								
C3									C54									D49									E30									F25								
C4									C55									D50									E31									F26								
C5									C56									D51									E32									F27								
C6									D1									D52									E33									F28								
C7									D2									D53									E34									G1								
C8									D3									D54									E35									G2								
C9									D4									D55									E36									G3								
C10									D5									D56									E37									G4								
C11									D6									D57									E38									G5								
C12									D7									D58									E39									G6								
C13									D8									D59									E40									G7								
C14									D9									D60									E41									G8								
																																					H1								